Scientific Journal of Informatics
Vol. 12, No. 3, August 2025
p-ISSN 2407-7658 https://journal.unnes.ac.id/journals/sji/index e-ISSN 2460-0040

MoLLe: A Hybrid Model for Classifying Diseases in Chili Plants Using Leaf Images

Itsnaini Irvina Khoirunnisa[1], Abdul Fadlil[2], Herman Yuliansyah[3*]
[1]Master Program of Informatics, Universitas Ahmad Dahlan, Indonesia
[2]Department of Electrical Engineering, Universitas Ahmad Dahlan, Indonesia
[3]Department of Informatics, Universitas Ahmad Dahlan, Indonesia

Abstract.
Purpose: Leaf diseases are often early indicators of problems in plants. More detailed image information with feature extraction on leaves can improve accuracy. However, MobileNetV2 tends to be less than optimal in capturing the fine texture characteristics of leaves. This research aims to propose a classification model for diseases in chili plants based on leaf images using MobileNetV2 with Local Binary Pattern (LBP), with three fully connected layers (220-120-60 neurons) using the ReLU activation function, referred to as MoLLe.
Methods: This research consists of six stages. It begins with a dataset collected from chili farms comprising 900 images, which are then preprocessed into 3,600 images. Next, LBP feature extraction is performed. After that, a comparison between the benchmark architecture and the proposed architecture is conducted. A softmax layer is used to perform three-class classification. The MoLLe model was tested with the MobileNetV2 and MobileNetV2+LBP benchmark architectures and evaluated using a confusion matrix.
Result: Based on the evaluation conducted, using batch size 32, learning rate 0.001, and 20 epochs, the MoLLe model experienced early stopping at epoch 11, achieving an accuracy of 0.97 training data, 0.84 validation data, and 0.91 testing data. The evaluation results showed consistent precision, recall, and F1-score values of 0.91, indicating the model's balanced ability to identify the three disease classes.
Novelty: The novelty of this research lies in the integration of MobileNetV2 and LBP with modifications to three fully connected layers, which not only reduces the number of training parameters but also accelerates the detection process. This research makes an essential contribution to the development of more efficient and effective plant disease detection systems, with experimental results showing that MoLLe outperforms the benchmark architecture.

Keywords: Disease detection, Image classification, Local binary pattern, MobileNetV2, Transfer learning
Received June 2025 / **Revised** July 2025 / **Accepted** August 2025

INTRODUCTION

Artificial intelligence (AI) has become a significant influence in many parts of everyday life, including technology, health, and agriculture [1]. The use of AI has spread to multiple sectors, such as object identification, where this technology is used to recognize Javanese characters [2]. Additionally, AI is used for classifying waste, such as plastic bottles [3] and visual pollutants [4], as well as in art classification, such as batik patterns [5] and Toraja wood carving motifs [6]. In healthcare, AI assists in body anatomy classification and brain tumor detection, thereby accelerating the diagnostic process [7]. However, in the agricultural sector, challenges remain, particularly in detecting diseases on chili leaves using image analysis. Traditional methods are typically used to record the severity of chili plant diseases based on visual observation [8].

Chili plants (*Capsicum sp*) is one of the most popular spices around the world [9]. Specifically, bird's eye chili (*Capsicum frutescens L*) plays an essential economic role in Indonesia due to its widespread distribution. All plants, including chili, are susceptible to various diseases that can cause crop failure, particularly triggered by weather factors such as rainfall and humidity [10]. However, in agriculture, there are still significant challenges in detecting diseases on chili leaves, as traditional methods are still used, which are subjective and inaccurate. This approach relies on visual observation by experts, which is costly and time consuming [11]. As a result, disease symptoms are often detected too late, leading to significant

*Corresponding author.
Email addresses: herman.yuliansyah@tif.uad.ac.id (Yuliansyah)
DOI: 10.15294/sji.v12i3.29071

losses in crop yield [12]. Detecting and recognizing plant diseases is crucial because it allows for monitoring large agricultural areas and quickly identifying disease symptoms as they appear on plant leaves [13]. Various AI techniques have been applied to detect and classify plant diseases, such as transfer learning. Transfer learning models, such as VGGNet, AlexNet, MobileNet, and ResNet, have been widely used to address various problems [14].

M. A. Berbar [15] presented the detect and evaluate diabetic retinopathy using the Messidor2 and EyePACS databases, achieving accuracies of 98.37% and 98.84%, respectively. The accuracy values obtained depend on the selection of pairs during Local Binary Pattern (LBP) feature extraction. Research shows that this method has a good ability to detect diabetic retinopathy because it can highlight the main features of images using a large dataset. P. F. Johari et al. [16] classified corn leaf diseases using a CNN with various color features, including GLCM, HSV, and L*a*b*. This research obtained 92.48% accuracy for corn leaf disease classification by combining HSV and L*a*b* color spaces in a CNN framework, outperforming GLCM-based combinations 91.75% for GLCM+L*a*b* and 90.29% for GLCM+HSV, confirming the advantage of fused color-brightness features.

S. Iqbal and A. N. Qureshi [17] estimated mitotic cores in breast cancer to determine tumor aggressiveness using DCCN and LBP. The proposed model achieved an F1-score of 95%, with sensitivity and specificity of 95%, and an area under the curve of 95%. Thus, these results can be used to develop a pathology tool in the medical field. S. Alsubai [18] identified lung and colorectal cancers using a ResNetV2 model integrated with strategic LPB feature extraction to improve accuracy. The model was trained using histopathological images and demonstrated an accuracy of 99.98%. These results have the potential to revolutionize more accurate and reliable cancer diagnosis. S. Tresnawati and H. Alfianti [19] improved brain tumor detection by combining Fuzzy Logic and K-fold validation to enhance classification accuracy and robustness. Images were analyzed using GLCM extraction to recognize textures in medical image interpretation. The proposed method achieved an accuracy of 99.88% in the K-fold validation process. These results can improve diagnostic precision and help overcome difficulties in distinguishing between different types of MRI tumor images.

Although many studies have used CNN-based classification techniques and LBP feature extraction in medical fields such as diabetic retinopathy detection [15], breast cancer [17], and lung and colon cancer [18], this approach has never been applied explicitly to chili leaf disease and the selected architecture configuration, making this research unique. Leaves play a crucial role in plant health as they are sensitive to climate changes and disease attacks [20], [21]. In chili plants, disease symptoms typically appear on leaves earlier than other plant parts [22], making leaves a focal point for disease detection. Chili leaf diseases often share similar symptoms, and feature extraction can help distinguish between them. This research proposed a method for classifying chili plant diseases by utilizing leaf images using MobileNetV2 and LBP, called MoLLe. In this combination, MobileNetV2 is used to extract deep features from images, while LBP captures local textures from images. This research successfully accelerates disease recognition and reduces the number of parameters [17]. The MoLLe model approach enables more detailed recognition of chili leaf disease image textures by leveraging the strengths of both methods.

METHODS

This section explains in detail how to achieve the performance results of the MoLLe model in chili leaf disease classification.

Research design

The research design outlines the research steps, starting from data collection, preprocessing, comparing benchmark architectures and the proposed architecture, classification, and evaluating the model's performance, as shown in Figure 1. This research uses three models: MoLLe, MobileNetV2+LBP, and MobileNetV2. Each model has different operational mechanisms and characteristics.

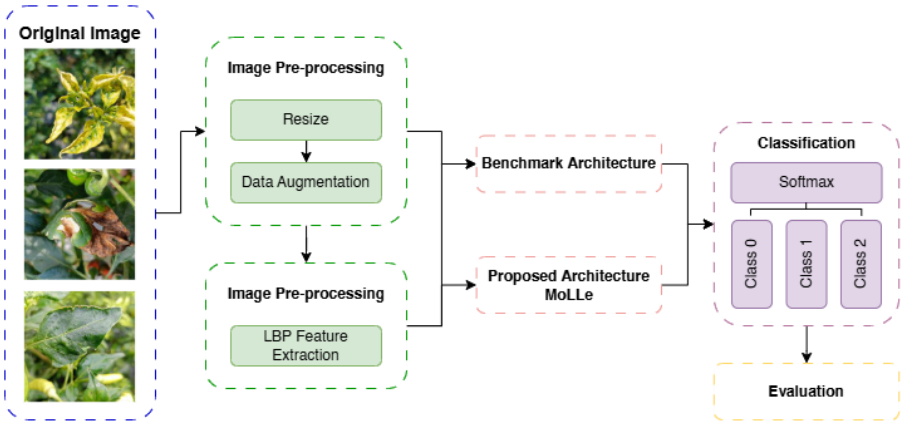

Figure 1. Research design

Dataset

The dataset was taken directly from chili plantations with 300 images per class before augmentation. To increase the amount of data, augmentation techniques were applied, including rotation, flipping, and cropping. Examples of images from each class can be seen in Figure 2.

(a) *Begomovirus* (b) Leaf spot (c) Healthy leaves

Figure 2. Representative leaf image samples from each disease class in the chili plant dataset

The proposed architecture

The MoLLe model, which combines MobileNetV2 and LBP features, is illustrated in Figure 3. This model produces a distinctive representation of chili leaf disease images. MobileNetV2 captures the deep features of the image [23], while LBP focuses on local texture extraction [24]. In this research, features from LBP are used together with features from MobileNetV2, which are combined using the concatenation method, thereby forming a more complete feature. After being combined, normalization is performed so that both methods are balanced. Additionally, the softmax function is applied to classify chili diseases based on the obtained characteristics. The classification results are then evaluated using a confusion matrix to determine the accuracy and effectiveness of the model in detecting diseases. This research addresses the shortcomings that have never been specifically used in classifying chili leaf diseases by combining MobileNetV2 and LBP. This is important because chili leaves tend to illustrate disease symptoms earlier than other parts. This approach differs from existing methods because it combines the advantages of both methods, so it can improve classification accuracy compared to methods that only use one method.

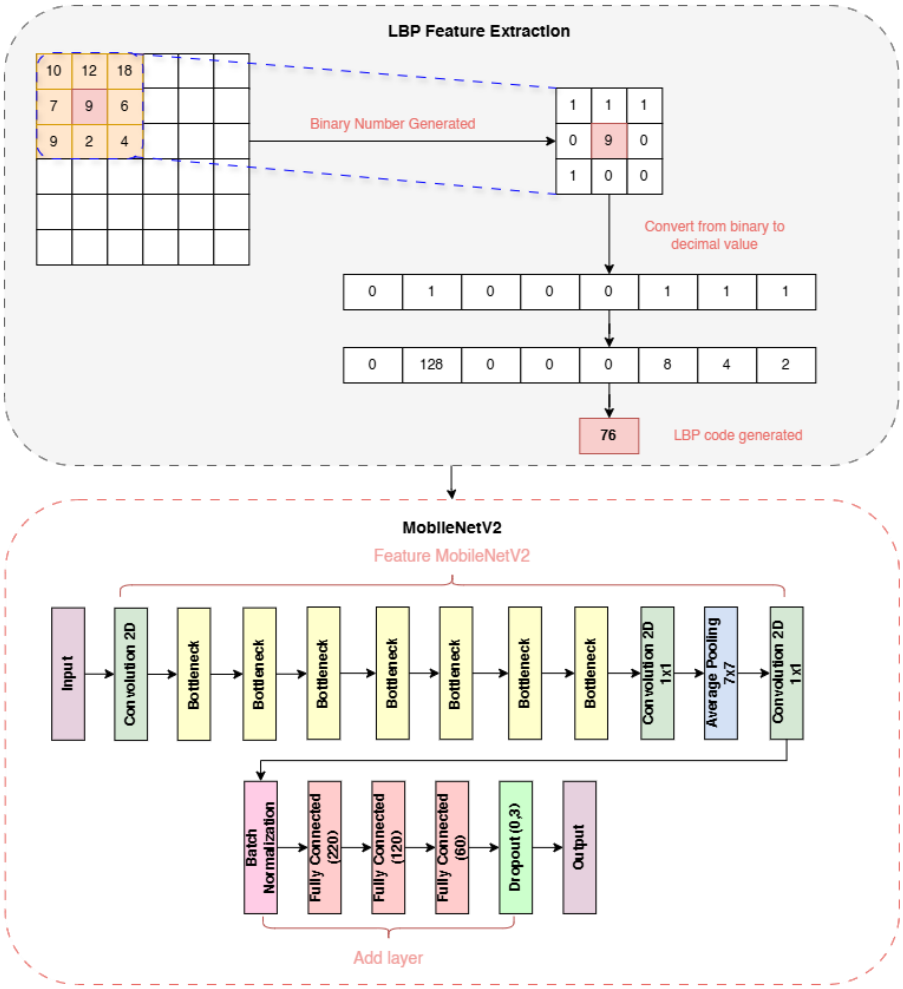

Figure 3. The proposed architecture MoLLe

Figure 3 illustrates the structure of the MoLLe model, which is divided into two parts, namely LBP extraction and MobileNetV2. The LBP part extracts texture features from leaf images using a 3×3 window by comparing the center pixel with its eight neighbors, resulting in a binary code in decimal numbers to obtain the LBP code. The MobileNetV2 component begins with the leaf image input layer, followed by a 2D convolution layer. The seven bottleneck layers play a crucial role in feature extraction using convolution techniques. Subsequently, the original architecture is augmented with three fully connected layers and dropout, processed to gather essential information and transform it into more complex features, thereby generating output aligned with the predicted results.

Benchmark architecture

This section describes the benchmark architecture used, focusing on two models, MobileNetV2+LBP and MobileNetV2. These two models are designed to be compared with the proposed model to solve the problem of classifying diseases in chili leaves, but using different approaches.

MobileNetV2+LBP

Figure 4 illustrates the architecture that integrates LBP with MobileNetV2 without adding additional layers, aiming to improve the model's ability to extract texture and pattern features from chili leaf images. The LBP block extracts feature from leaf images, where each central pixel is compared with eight neighbouring pixels. The MobileNetV2 block captures deep features through efficient 2D convolution and bottleneck layers, followed by an average pooling layer to reduce feature dimensions.

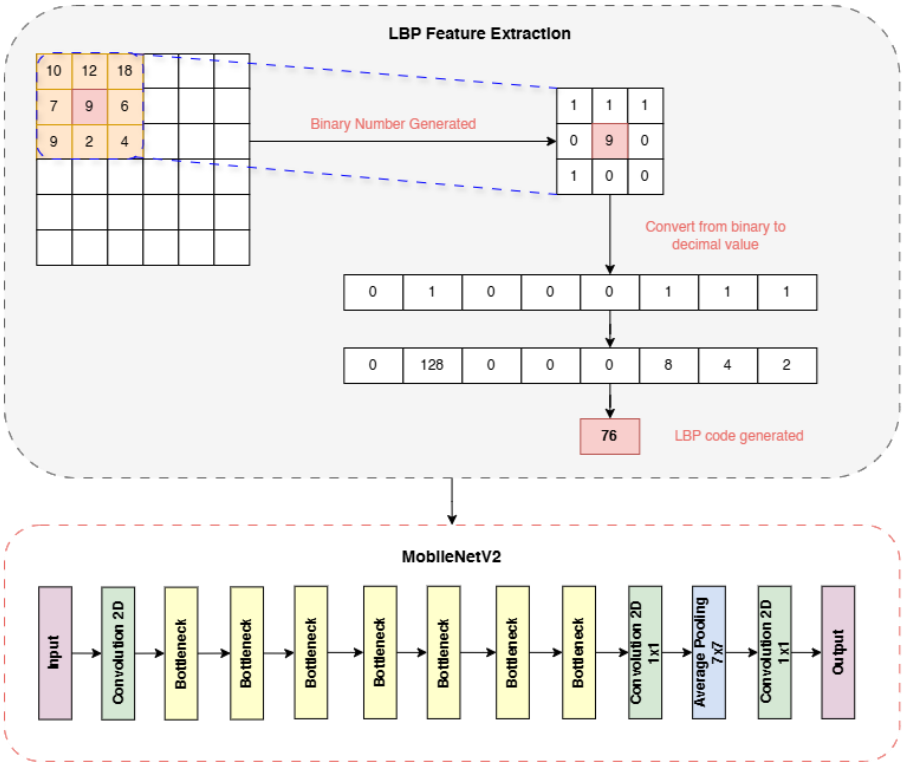

Figure 4. Architecture MobileNetV2+LBP

MobileNetV2

This architecture uses MobileNetV2 without the LBP process during the preprocessing stage. This model focuses on deep feature extraction from images using the basic MobileNetV2 architecture. This MobileNetV2 block is the same as the MobileNetV2 block shown in Figure 4. The architectural representation can be seen in Figure 5.

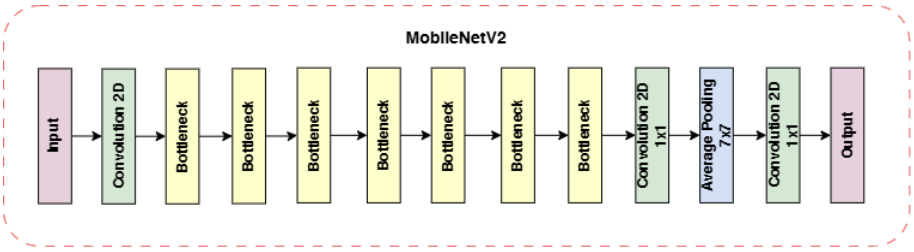

Figure 5. Architecture MobileNetV2

Local binary pattern

LBP is considered one of the strongest feature extraction methods [25] and was first introduced by Ojala et al. to represent the local features of an image [26]. The original LBP operator uses a 3×3 pixel window to assign labels to pixels, and the central pixel value sets the threshold [27]. The three neighboring pixels provide $2^8 = 256$ levels to form a histogram as a feature map, as shown in Equation 1 [28].

$$LBP_{I,J}(g_c) = \sum_{j=0}^{J-1} G(g_j - g_c)2^j \quad (1)$$

where

$$G(m) = \begin{cases} 0, & m < 0 \\ 1, & otherwise \end{cases} \quad (2)$$

In Equation (1), $g_j = g(m,n)$ is the central pixel at position (m,n) dan $g_j = g(m_j, n_j)$ is the neighboring pixel of the central pixel g_c [8].

MobileNetV2

MobileNetV2 features an inverted residual architecture with linear bottlenecks, which help reduce convolution computations [1]. Its architecture is simpler and has better memory efficiency [29]. The input image thickness is adjusted to match the filter thickness in MobileNetV2 [30]. Figure 3 shows the MoLLe model for classifying chili plant leaf diseases. The proposed MoLLe architecture processes 224 × 224 pixels normalized images through 3×3 convolutional kernels, followed by a fully connected network structure (220-120-60 neurons), culminating in a neuron classification layer for disease class output.

Dropout serves as a neural network regularization method that randomly deactivates neurons during training to prevent overfitting [31]. The MoLLe model uses a dropout value of 0.3. The convolutional layer and fully connected layer in this model use the ReLu activation function, which provides significantly faster computation speed [32]. In the final stage, the softmax function is used to handle multi-class classification [33]. Thus, the use of deeper convolutional layers and the selection of appropriate model parameters enable high accuracy and improved computational efficiency [34].

Evaluation

In evaluating the performance of this research, a confusion matrix was used to analyze the classification results. The values of true positive (TP), false positive (FP), true negative (TN), and false negative (FN) were used to calculate accuracy, precision, recall, and F1-Score [18]. Accuracy measures how many correct predictions the model makes [35].

$$accuracy = \frac{TP+TN}{TP+TN+FP+FN} \quad (3)$$

Precision shows how many of the positive cases the model correctly found, compared to all the cases it said were positive [36].

$$precision = \frac{TP}{TP+FP} \quad (4)$$

Recall measures the model's ability to accurately identify positive cases in a particular class [37].

$$recall = \frac{TP}{TP+FN} \quad (5)$$

F1-Score is used to address the issue of class imbalance in data by combining precision and recall into a single score [38].

$$F1 - Score = \frac{2 \times Precision \times Recall}{Precision+Recall} \quad (6)$$

RESULTS AND DISCUSSIONS

Before the model training process, the chili leaf image dataset underwent data augmentation to increase sample variation. From the initial 900 images, transformations were performed with 90˚ rotation, horizontal and vertical flipping to add perspective variation, and cropping to take the central area of the leaf at 50% of the original size to ensure the model focused on pathological features in the central area of the leaf. This augmentation process produced 3,600 leaf images, as shown in Table 1. Next, LBP extraction can be seen in Figure 6.

Table 1. Number of images for each class in the chili plant leaf diseases dataset

No	Class	Samples	
		Before Augmentation	After Augmentation
1	Begomovirus	300	1,200
2	Leaf spot	300	1,200
3	Healthy leaves	300	1,200
Total		**900**	**3,600**

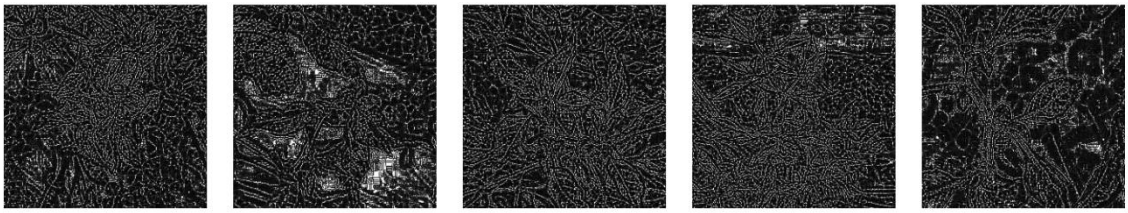

(a) Begomovirus

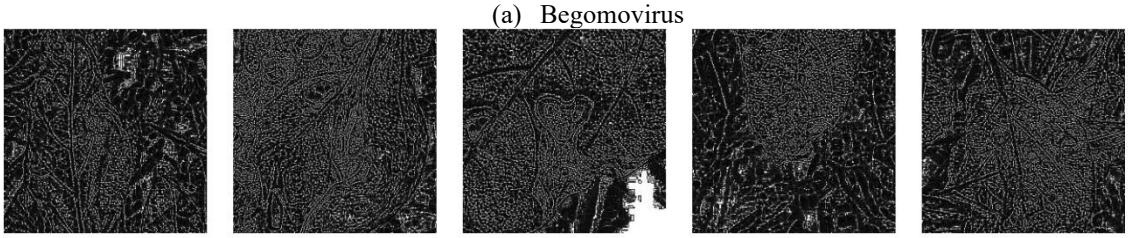

(b) Leaf spot

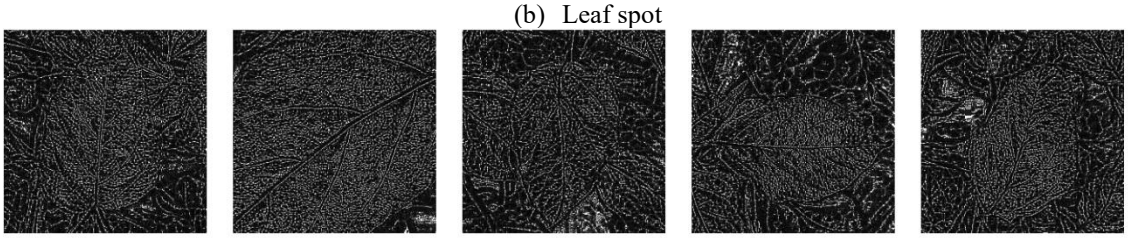

(c) Healthy leaves

Figure 6. (a), (b), and (c) examples of images that have undergone data augmentation and LBP extraction for each class

The division of the research dataset applies stratified sampling to ensure a balanced class distribution in each data subset. From a total of 3,600 images after augmentation, the dataset is divided into three parts: 70% for training, 20% for validation, and 10% for testing. This division is presented in Table 2. The hyperparameter configuration used includes a batch size of 32, a learning rate of 0.001, and 20 epochs. To prevent overfitting, an early stopping mechanism is applied, which automatically stops the training process when the model performance on the validation data does not show improvement after a certain number of epochs. This research proposed the MobileNetV2+LBP model by adding three fully connected layers (220, 120, and 60 neurons) using the ReLU activation function. The selection of this configuration is based on experiments that consider classification effectiveness, overfitting control, and computational efficiency. The addition of these layers optimizes the combination of LBP texture features with transfer learning features, enabling the model to distinguish visual characteristics between classes of chili plant diseases.

Table 2. Split dataset

Class	Training Data	Validation Data	Testing Data
Begomovirus	840	240	120
Leaf spot	840	240	120
Healthy leaves	840	240	120
Total	2,520	720	360
Total dataset	3,600		

The training process terminated at epoch 11 via early stopping, demonstrating optimal model convergence. Both training and validation loss exhibited substantial reduction throughout the learning period. The model achieved 0.97 training accuracy and 0.84 validation accuracy, reflecting strong pattern recognition capabilities. These learning dynamics are visualized in Figures 7 and 8.

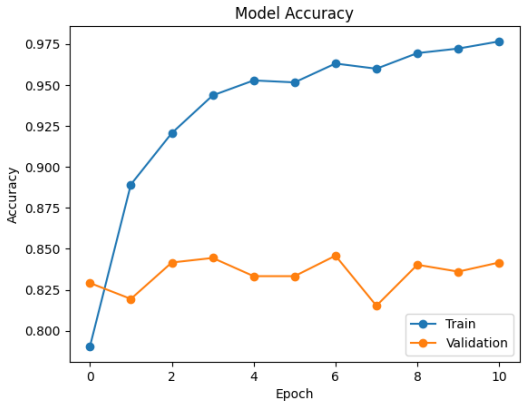

Figure 7. Model accuracy progression across training and validation datasets

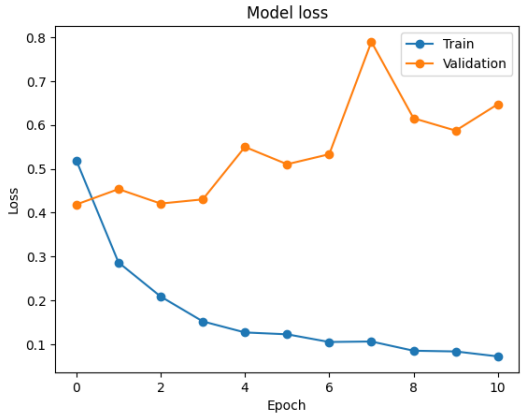

Figure 8. Loss function dynamics during model training and validation

The test results presented in Table 3 show that the MoLLe model successfully achieved an accuracy of 0.91 in classifying diseases on chili leaves. The consistent precision, recall, and F1-score values of 0.91 indicate that this model has a balanced ability to identify the three disease classes. These results are significantly better than those of comparison models such as MobileNetV2+LBP, which only achieved an accuracy of 0.59, and MobileNetV2, which achieved an accuracy of 0.74.

Table 3. Comparison of the proposed model and the MobileNetV2 based model

No	Model	Accuracy	Precision	Recall	F1-Score
1	**MoLLe**	**0.91**	**0.91**	**0.91**	**0.91**
2	MobileNetV2+LBP	0.59	0.73	0.59	0.59
3	MobileNetV2	0.74	0.81	0.74	0.70

Testing the MoLLe model with an external dataset showed high results. The model achieved an accuracy of 0.88. The precision, recall, and F1-score values were 0.87, 0.89, and 0.88, respectively, indicating that the model still performed well in identifying disease classes on chili leaves outside the testing data. These results confirm the generalization ability of the MoLLe model, despite some classification errors.

The results of the MoLLe model are consistent with the research [16] that used hybrid feature extraction on corn leaves, but the proposed model is superior in distinguishing fine textures due to the optimization of the convolutional layer and the 0.3 dropout mechanism that reduces overfitting. Comparison with previous studies reinforces the effectiveness of this approach. As another example, research [18] achieved 99.98% accuracy for cancer detection using ResNetV2 + LBP, but it used a more homogeneous histopathology dataset. Meanwhile, the proposed model successfully addressed illumination variations and complex backgrounds in chili leaf images due to data augmentation that improved generalization. However, the limited number of samples before the augmentation of 300 per class posed a challenge, as faced by [15] in retinopathy detection.

Figure 9 shows the performance of the MoLLe model in classifying disease classes, indicating that the model demonstrates a good ability to distinguish between healthy leaf and leaf spot classes, with low error rates in predicting each class. Although there are some misclassifications, particularly between the begomovirus and leaf spot classes, the model still achieves good results in classifying plant diseases. Figure 10 present the confusion matrix of the MobileNetV2+LBP model. The results indicate an accuracy of 0.59, which shows relatively low performance in classifying disease classes. The model has difficulty distinguishing between begomovirus and leaf spot classes, as seen in the high number of incorrect predictions for both classes.

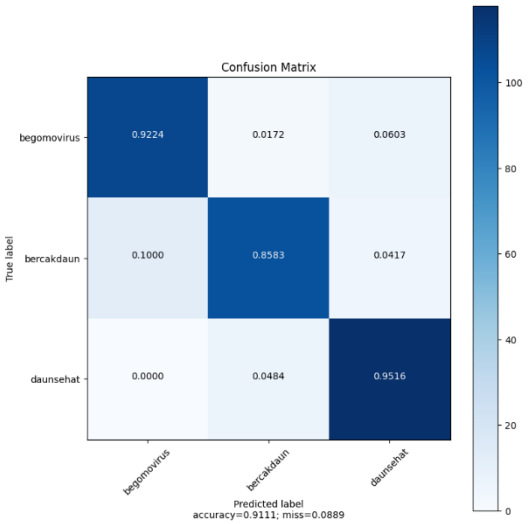

Figure 9. Confusion matrix of MoLLe

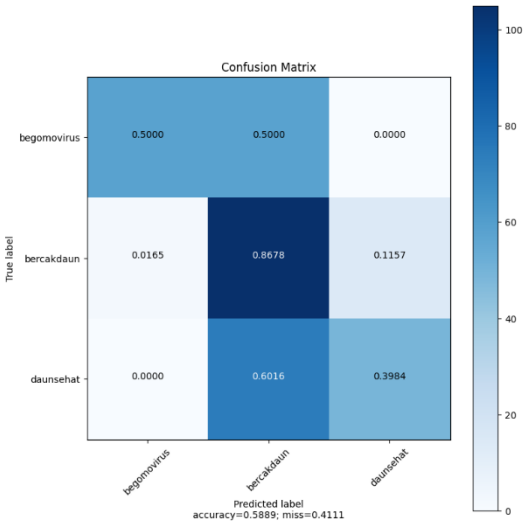

Figure 10. Confusion matrix of MobileNetV2+LBP

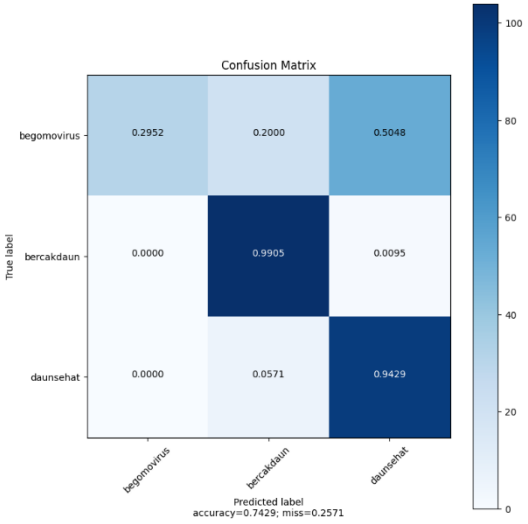

Figure 11. Confusion matrix of MobileNetV2

Figure 11 shows the confusion matrix of the MobileNetV2 model, where the accuracy results obtained are closer to the MoLLe model. There are several classification errors, particularly in the begomovirus class, which could be a focus area for improvement. These misclassifications indicate the complexity of distinguishing between classes with similar visual features. With an accuracy of 0.74, the MobileNetV2 model demonstrates good performance, although it falls short of the MoLLe model.

The MoLLe model integrates LBP and MobileNetV2 to enable simultaneous extraction of texture and pattern features. LBP captures local texture information, while MobileNetV2 focuses on extracting deep features from images. This combination offers advantages in detecting subtle variations in chili leaf images

and reduces overfitting through the dropout mechanism. The proposed method performs better because it combines the strengths of both approaches, resulting in a more complete and robust feature representation. The MoLLe model, with its impressive accuracy of 0.91 and precision and recall values also at 0.91, outshines the competition. In comparison, MobileNetV2+LBP only achieved 0.59, and MobileNetV2 achieved 0.74. The MoLLe model's ability to recognize all three classes of chili diseases is a testament to its robustness. Moreover, the MoLLe model's computing time of only 37 minutes and 19 seconds, compared to 3 hours, 32 minutes, and 18 seconds for MobileNetV2+LBP and 5 hours, 21 minutes, and 8 seconds for MobileNetV2, underscores its efficiency. In summary, the MoLLe model's high accuracy and efficient computing time, coupled with its lightweight architecture, position it as a superior option for detecting plant diseases, instilling confidence in its performance.

CONCLUSION

This research successfully developed the MoLLe model, which combines MobileNetV2 and LBP feature extraction by adding a fully connected layer to detect chili leaf diseases. The model produced a training accuracy of 0.97, a validation accuracy of 0.84, and a testing accuracy of 0.91. These results were better than the other two models. The MobileNetV2+LBP model had an accuracy of 0.59, while MobileNetV2 alone reached 0.74. However, both models have trouble telling begomovirus and leaf spot apart because they look very similar. This is the main issue that needs to be fixed in future work. Using dropout and improving the convolutional layer helped reduce overfitting, but more data is needed to make the model better at generalizing. This research shows great promise for disease detection in chili plants, helping farmers spot problems early and take action. For future research, it's suggested to collect more data for each class and use transfer learning from more advanced models.

REFERENCES

[1] Y. Gulzar, "Fruit Image Classification Model Based on MobileNetV2 with Deep Transfer Learning Technique," *Sustainability (Switzerland)*, vol. 15, no. 3, pp. 1–14, Feb. 2023, doi: 10.3390/su15031906.

[2] E. B. Sudewo, M. K. Biddinika, R. Umar, and A. Fadlil, "Evaluating the Impact of Optimizer Hyperparameters on ResNet in Hanacaraka Character Recognition," *Preservation, Digital Technology & Culture*, Feb. 2025, doi: 10.1515/pdtc-2024-0061.

[3] S. Chatterjee, D. Hazra, Y.-C. Byun, and Y.-W. Kim, "Enhancement of Image Classification Using Transfer Learning and GAN-Based Synthetic Data Augmentation," *Mathematics*, vol. 10, no. 9, p. 1541, May 2022, doi: 10.3390/math10091541.

[4] N. H. Tasnim, S. Afrin, B. Biswas, A. A. Anye, and R. Khan, "Automatic Classification of Textile Visual Pollutants Using Deep Learning Networks," *Alexandria Engineering Journal*, vol. 62, pp. 391–402, Jan. 2023, doi: 10.1016/j.aej.2022.07.039.

[5] M. Murinto and S. Winiarti, "Modified particle swarm optimization (MPSO) optimized CNN's hyperparameters for classification," *International Journal of Advances in Intelligent Informatics*, vol. 11, no. 1, p. 133, Feb. 2025, doi: 10.26555/ijain.v11i1.1303.

[6] N. Wardhani, B. E. W. Asrul, A. R. Tampang, S. Zuhriyah, and A. L. Arda, "Classification of Toraja Wood Carving Motif Images Using Convolutional Neural Network (CNN)," *Jurnal RESTI (Rekayasa Sistem dan Teknologi Informasi)*, vol. 8, no. 4, pp. 486–495, Aug. 2024, doi: 10.29207/resti.v8i4.5897.

[7] A. K. Aggarwal, "Learning Texture Features from GLCM for Classification of Brain Tumor MRI Images using Random Forest Classifier," *WSEAS TRANSACTIONS ON SIGNAL PROCESSING*, vol. 18, pp. 60–63, Apr. 2022, doi: 10.37394/232014.2022.18.8.

[8] K. M. Hosny, W. M. El-Hady, F. M. Samy, E. Vrochidou, and G. A. Papakostas, "Multi-Class Classification of Plant Leaf Diseases Using Feature Fusion of Deep Convolutional Neural Network and Local Binary Pattern," *IEEE Access*, vol. 11, pp. 62307–62317, Jun. 2023, doi: 10.1109/ACCESS.2023.3286730.

[9] J. A. Sosa-Herrera, N. Alvarez-Jarquin, N. M. Cid-Garcia, D. J. López-Araujo, and M. R. Vallejo-Pérez, "Automated Health Estimation of Capsicum annuum L. Crops by Means of Deep Learning and RGB Aerial Images," *Remote Sens (Basel)*, vol. 14, no. 19, pp. 4943–4966, Oct. 2022, doi: 10.3390/rs14194943.

[10] W. Andini, S. K. Zahra, M. Abdurrahman, and V. B. Sebayang, "Analisis Fluktuasi Harga Terhadap Faktor-Faktor yang Mempengaruhi Produktivitas Usaha Tani Cabai Merah di Indonesia," *Jurnal Riset dan Inovasi Manajemen*, vol. 2, no. 2, pp. 162–172, May 2024, doi: 10.59581/jrim-widyakarya.v2i2.3526.

[11] H. Tariq *et al.*, "Current Status of Yam Diseases and Advances of Their Control Strategies," *Agronomy*, vol. 14, no. 7, p. 1575, Jul. 2024, doi: 10.3390/agronomy14071575.
[12] J. Schmitt, F. Offermann, M. Söder, C. Frühauf, and R. Finger, "Extreme weather events cause significant crop yield losses at the farm level in German agriculture," *Food Policy*, vol. 112, p. 102359, Sep. 2022, doi: 10.1016/j.foodpol.2022.102359.
[13] A. S. Paymode and V. B. Malode, "Transfer Learning for Multi-Crop Leaf Disease Image Classification using Convolutional Neural Network VGG," *Artificial Intelligence in Agriculture*, vol. 6, no. 1, pp. 23–33, Jan. 2022, doi: 10.1016/j.aiia.2021.12.002.
[14] B. Ramamurthy and S. Prakash, "Gray Level Co-occurrence Matrix based Fully Convolutional Neural Network Model for Pneumonia Detection," *International journal of electrical and computer engineering systems*, vol. 15, no. 4, pp. 369–376, Mar. 2024, doi: 10.32985/ijeces.15.4.7.
[15] M. A. Berbar, "Features Extraction Using Encoded Local Binary Pattern for Detection and Grading Diabetic Retinopathy," *Health Inf Sci Syst*, vol. 10, no. 1, p. 14, Jun. 2022, doi: 10.1007/s13755-022-00181-z.
[16] P. F. Johari, N. Arifin, and M. S. A. Utama, "Corn Leaf Diseases Classification Using CNN with GLCM, HSV, and L*a*b* Features," *Jurnal Teknik Informatika (JUTIF)*, vol. 6, no. 2, pp. 709–722, 2025, doi: 10.52436/1.jutif.2025.6.2.4345.
[17] S. Iqbal and A. N. Qureshi, "A Heteromorphous Deep CNN Framework for Medical Image Segmentation Using Local Binary Pattern," *IEEE Access*, vol. 10, pp. 63466–63480, Jun. 2022, doi: 10.1109/ACCESS.2022.3183331.
[18] S. Alsubai, "Transfer Learning Based Approach for Lung and Colon Cancer Detection Using Local Binary Pattern Features and Explainable Artificial Intelligence (AI) Techniques," *PeerJ Comput Sci*, vol. 10, p. e1996, Apr. 2024, doi: 10.7717/peerj-cs.1996.
[19] S. Tresnawati and H. Alfianti, "Brain Tumor Detection Using Improved Fuzzy Logic Classifier Model Based on K-folds Validation," *Scientific Journal of Informatics*, vol. 11, no. 4, pp. 1005–1014, Feb. 2025, doi: 10.15294/sji.v11i4.13964.
[20] A. K.S., R. P. Singh, M. K. Panda, and K. Palaniappan, "An Ensemble Approach using Self-attention based MobileNetV2 for SAR classification," *Procedia Comput Sci*, vol. 235, pp. 3207–3216, 2024, doi: 10.1016/j.procs.2024.04.303.
[21] S. Mostafa, Y. Wang, W. Zeng, and B. Jin, "Plant Responses to Herbivory, Wounding, and Infection," *Int J Mol Sci*, vol. 23, no. 13, p. 7031, Jun. 2022, doi: 10.3390/ijms23137031.
[22] D. W. Rustanto, F. Liantoni, and N. P. T. Prakisya, "Identifikasi Penyakit Daun pada Tanaman Padi Menggunakan Ekstraksi Fitur Gray Level Co-occurrence Matrix (GLCM) dan Metode K-Nearest Neighbour (KNN)," *Jurnal Sistem dan Teknologi Informasi (JustIN)*, vol. 12, no. 1, pp. 100–106, Jan. 2024, doi: 10.26418/justin.v12i1.69752.
[23] C. Aydin, "Enhanced Material Classification via MobileSEMNet: Leveraging MobileNetV2 for SEM Image Analysis," *Traitement du Signal*, vol. 40, no. 6, pp. 2779–2787, Dec. 2023, doi: 10.18280/ts.400638.
[24] Z. Pan, S. Hu, X. Wu, and P. Wang, "Adaptive Center Pixel Selection Strategy in Local Binary Pattern for Texture Classification," *Expert Syst Appl*, vol. 180, p. 115123, Oct. 2021, doi: 10.1016/j.eswa.2021.115123.
[25] Y. ELsayed, A. ELSayed, and M. A. Abdou, "An automatic improved facial expression recognition for masked faces," *Neural Comput Appl*, vol. 35, no. 20, pp. 14963–14972, Jul. 2023, doi: 10.1007/s00521-023-08498-w.
[26] T. Ojala, M. Pietikainen, and D. Harwood, "Performance evaluation of texture measures with classification based on Kullback discrimination of distributions," in *Proceedings of 12th International Conference on Pattern Recognition*, IEEE Comput. Soc. Press, 1994, pp. 582–585. doi: 10.1109/ICPR.1994.576366.
[27] N. Carbone, L. Bernini, P. Albertelli, and M. Monno, "Assessment of milling condition by image processing of the produced surfaces," *The International Journal of Advanced Manufacturing Technology*, vol. 124, no. 5–6, pp. 1681–1697, Jan. 2023, doi: 10.1007/s00170-022-10516-5.
[28] K. M. Hosny, W. M. El-Hady, F. M. Samy, E. Vrochidou, and G. A. Papakostas, "Multi-Class Classification of Plant Leaf Diseases Using Feature Fusion of Deep Convolutional Neural Network and Local Binary Pattern," *IEEE Access*, vol. 11, pp. 62307–62317, 2023, doi: 10.1109/ACCESS.2023.3286730.
[29] M. Alkanan and Y. Gulzar, "Enhanced Corn Seed Disease Classification: Leveraging MobileNetV2 with Feature Augmentation and Transfer Learning," *Front Appl Math Stat*, vol. 9, no. 1, pp. 1–12, Jan. 2024, doi: 10.3389/fams.2023.1320177.

[30] A. N. M. Ramadhani, G. W. Saraswati, R. T. Agung, and H. A. Santoso, "Performance Comparison of Convolutional Neural Network and MobileNetV2 for Chili Diseases Classification," *Jurnal RESTI (Rekayasa Sistem dan Teknologi Informasi)*, vol. 7, no. 4, pp. 940–946, Aug. 2023, doi: 10.29207/resti.v7i4.5028.

[31] I. Salehin and D.-K. Kang, "A Review on Dropout Regularization Approaches for Deep Neural Networks within the Scholarly Domain," *Electronics (Basel)*, vol. 12, no. 14, p. 3106, Jul. 2023, doi: 10.3390/electronics12143106.

[32] Y. Wang, Y. Li, Y. Song, and X. Rong, "The Influence of the Activation Function in a Convolution Neural Network Model of Facial Expression Recognition," *Applied Sciences*, vol. 10, no. 5, p. 1897, Mar. 2020, doi: 10.3390/app10051897.

[33] Q. A. Fitroh and S. 'Uyun, "Deep Transfer Learning untuk Meningkatkan Akurasi Klasifikasi pada Citra Dermoskopi Kanker Kulit," *Jurnal Nasional Teknik Elektro dan Teknologi Informasi*, vol. 12, no. 2, pp. 78–84, May 2023, doi: 10.22146/jnteti.v12i2.6502.

[34] L. Chen, S. Li, Q. Bai, J. Yang, S. Jiang, and Y. Miao, "Review of Image Classification Algorithms Based on Convolutional Neural Networks," *Remote Sens (Basel)*, vol. 13, no. 22, p. 4712, Nov. 2021, doi: 10.3390/rs13224712.

[35] V. Chang, M. A. Ganatra, K. Hall, L. Golightly, and Q. A. Xu, "An Assessment of Machine Learning Models and Algorithms for Early Prediction and Diagnosis of Diabetes Using Health Indicators," *Healthcare Analytics*, vol. 2, p. 100118, Nov. 2022, doi: 10.1016/j.health.2022.100118.

[36] W. Lin, H. Yu, and L. Wang, "A Data-Driven Deep Learning Approach Incorporating Investor Sentiment and Government Interventions to Predict Post-Crash Stock Return in China's A-share Market," *Journal of Innovation & Knowledge*, vol. 10, no. 3, p. 100704, May 2025, doi: 10.1016/j.jik.2025.100704.

[37] M. Meral, F. Ozbilgin, and F. Durmus, "Fine-Tuned Machine Learning Classifiers for Diagnosing Parkinson's Disease Using Vocal Characteristics: A Comparative Analysis," *Diagnostics*, vol. 15, no. 5, p. 645, Mar. 2025, doi: 10.3390/diagnostics15050645.

[38] S. Seo *et al.*, "Predicting Successes and Failures of Clinical Trials With Outer Product–Based Convolutional Neural Network," *Front Pharmacol*, vol. 12, no. 670670, Jun. 2021, doi: 10.3389/fphar.2021.670670.